Building Tomorrow's Society
Bâtir la Société de Demain

Fredericton, Canada
June 13 – June 16, 2018/ *Juin 13 – Juin 16, 2018*

INVESTIGATION OF WATER FLOW PASSING UNDERNEATH A SLUICE GATE BY EXPERIMENTAL AND NUMERICAL METHODS

Xu, Bowen[1], Li, Samuel[2,3]
[1] Graduate Student, Dept. of Building, Civil and Environmental Engineering
Concordia Univ., 1455 de Maisonneuve Blvd. W., Montreal, QC, Canada H3G 1M8
[2] Professor, Dept. of Building, Civil and Environmental Engineering
Concordia Univ., 1455 de Maisonneuve Blvd. W., Montreal, QC, Canada H3G 1M8
[3] (Corresponding author). E-mail: sam.li@concordia.ca

Abstract: Sluice gates are useful for the control of discharge and flow level in water and wastewater facilities. The purpose of this paper is to investigate the characteristics of highly curved flow immediately downstream from a vertical sluice gate. This paper takes the experimental and numerical approaches. Laboratory experiments as well as numerical simulations of sluice gate flow were carried out under the conditions of gate opening equal to 2.54, 3.81 and 5.08 cm (or 1, 1.5 and 2 inches), and upstream-flow-depth to gate-opening ratio ranging from 10.16 to 40.64 cm (or 4 to 16 inches). The simulations use the Reynolds-averaged Navier-Stokes equations for two-phase flow, SST k-ω model for turbulence closure, and the volume of fluid method for free surface tracking. Using OpenFOAM as a solver, the model equations are numerically solved for finite volume solutions of flow velocity and pressure. The experiments and simulations produce results of flow profiles, contraction length, contraction coefficient, distributed pressures on the gate surface and at the channel-bed, and flow curvature. The numerical results compare well with the experimental data. Further simulations were carried at large gate openings (10.16, 20.32, and 40.64 cm) to investigate variations in flow curvature under field conditions. The SST k-ε model is a better choice than the standard k-ε model for turbulence closure. This paper extends previous research of sluice gate flow and contributes to an improved understanding of highly curved flows passing underneath a sluice gate. Suitable simulation strategies are discussed.

1 INTRODUCTION

In Hydraulic Engineering, sluice gates are a useful structure for the control of discharge and water level. A good understanding of the characteristics of sluice gate flow is essential for the optimal design and safe operations of sluice gates. To simplify the analysis of the flow, previous studies have used a number of assumptions: 1) The flow is steady, incompressible, and frictionless; 2) The flow is one-dimensional, with straight streamlines and without turbulent velocity fluctuations; 3) The flow is uniform at cross sections a short distance upstream as well as downstream from the gate section; 4) The associated pressure is hydrostatic. Some of them are invalid for the flow immediately downstream from the gate section.

According to Frisch et al. (2004), when the ratio of the upstream flow depth, y_1, to the sluice gate opening, w, is large, the flow velocity at the vena contracta, v_2, can be expressed as

[1] $$v_2 = \sqrt{2g(y_1 - y_{2c})}$$

where g is gravity; y_{2c} is the flow depth at the vena contracta. A contraction coefficient is defined as

[2] $C_c = y_{2c}/w$

This is an important parameter for the analysis of discharge. The determination of C_c has received substantial attention from previous researchers. The per-unit-width discharge can be expressed as:

[3] $q = C_c w\sqrt{2g(y_1 - C_c w)}$

The effect of the approach flow velocity head ${v_1}^2/2g$ on v_2 and hence on q has been ignored in Equations [1] and [3], which causes underestimates of v_2 and q. Henderson (1966, p. 203) rewrote Equation [3] as:

[4] $q = C_d w\sqrt{2gy_1}$

where C_d is the discharge coefficient, calculated as $C_d = C_c/\sqrt{1 + C_c w/y_1}$. Equation [4] allows for the effect of v_1 (Chow, 1959, p. 509).

Previously, experimental and numerical investigations of flow passing underneath a sluice gate have focused on the contraction coefficient. In the literature, C_c varies from 0.59 to 0.75, with an asymptotic value of 0.61. The coefficient appears to increase with increasing y_1/w and the Froude number Fr. Here, Fr is evaluated at the vena contracta.

Another important aspect of the sluice gate problem is the characteristics of highly curved flow immediately downstream from the gate. To the best of our knowledge, this has not been studied adequately. The purpose of this paper is to improve our understanding of flow profile, contraction length, contraction coefficient, distributed pressures, and flow curvature.

In the following, Section 2 describes laboratory experiments of sluice gate flow conducted in Water Resources Engineering Laboratory at Concordia University. Section 3 is devoted to numerical simulations of the flow using OpenFOAM (an open-source CFD software). Section 4 discusses the experimental and numerical results, before conclusions drawn in Section 5.

2 FLUME EXPERIMENTS

Experiments of flow passing underneath a sluice gate were performed using a laboratory flume (Figure 1). During the experiments, flow discharge, pressure distribution, and downstream flow surface profile were measured.

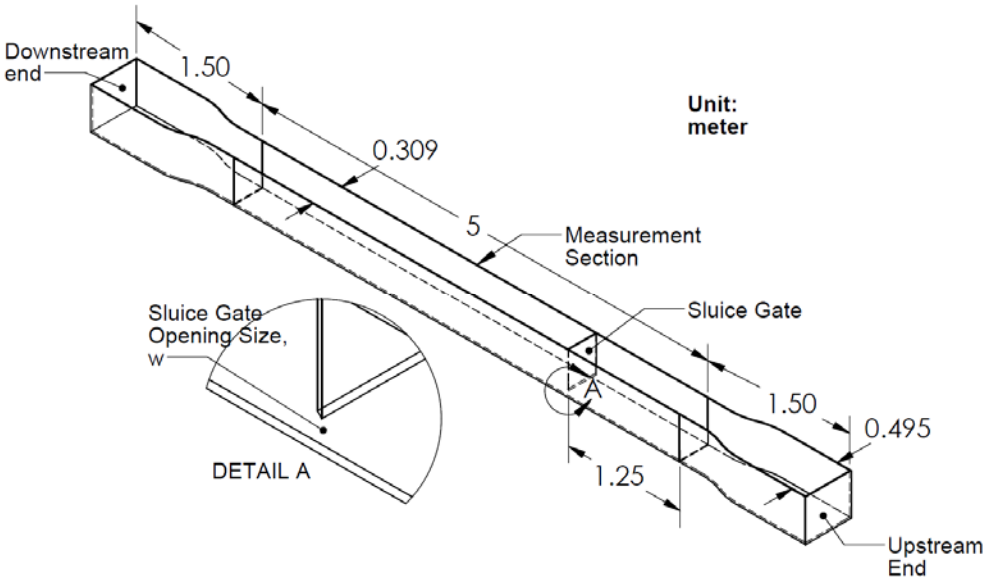

Figure 1: Diagram of the laboratory flume used in this study

The experiments used three different gate openings: w = 2.54, 3.81 and 5.08 cm (or 1, 1.5 and 2 inches). The discharge, Q, was adjusted to obtain desirable upstream flow depth, y_1, and thus different y_1/w. Twenty five distinct hydraulic conditions for the experiments is summarised in Table 1. For each of these conditions, five duplicated experiments were performed to quantify experimental errors. Thus, a total of 125 experiments were performed in this study.

Table 1: Distinct hydraulic conditions for experiments of flow. The Froude number at the vena contracta is determined, assuming a contraction coefficient of 0.62. The contraction distance, x_c, is the longitudinal distance from the gate opening to the vena contracta.

Gate opening w (cm)	y_1/w	Discharge Q (L/s)	Fr	Observed x_c/w	Predicted x_c/w
2.54	4,5,6,…,16	4.55 to 13.60	3.144 to 6.775	1.575	1.772
3.81	4,5,6,…,10	11.89 to 19.68	2.756 to 4.552	1.470	1.470
5.08	4,5,6,…,8	18.14 to 26.65	1.649 to 2.390	1.575	1.535

The pressures on the gate surface were measured by using manometers, with taps installed along the vertical centreline. The vertical distances of these taps were 0.32, 0.96, 1.6, 2.87, 5.41, 10.49, 15.57, 20.65, 25.73, and 30.81 cm above the lower edge of the sluice gate.

The positions of the free water surface were measured using point gauges. The accuracy is ±0.1 mm. These measurements were made along the flume centreline. The flow discharges were obtained from an electromagnetic flowmeter.

3 NUMERICAL MODEL

Numerical simulations were carried out for the same hydraulic conditions as the laboratory experiments (Table 1). The numerical model is based on the Reynolds-averaged continuity and Navier- Stokes equations for two-phase turbulent flow, with air being the gas phase and water as the liquid phase. The flow is incompressible. In tensor notion, the model equations are of the form:

[4] $\frac{\partial u_i}{\partial x_i} = 0$

[5] $\rho u_j \frac{\partial u_i}{\partial x_j} = \rho K_i - \frac{\partial p}{\partial x_i} + \mu \frac{\partial^2 u_i}{\partial x_j \partial x_j} + \frac{\partial}{\partial x_j}(-\rho \overline{u_i' u_j'})$

where ρ is the density of the air-water mixture; u_i is the velocity component of the fluid mixture in the x_i-direction; K_i is the body force generated by gravity; p is the pressure; μ is the dynamic viscosity of the fluid mixture.

The volume of fluid method is used to trace the air-water interface. The two-equation SST k-ω model is used for turbulence closure. Some simulations were carried out using the two-equation standard k-ε model for turbulence closure. The idea is to compare the suitability of the two turbulence closure models.

The model equations are numerically solved using the finite volume methods. This involves discretising the model channel (Figure 2) into high resolution cells. For a balanced computing efficiency and numerical accuracy, the mesh covers the channel with square cells of 0.01-cm resolution, with resolution refinement of five layers next to the channel-bed and gate surface. The thickness of these layers is limited to 0.005 cm. This ensures that the first cell off the bed and gate surface falls in the logarithmic layer, and the associated wall distance is $30 < y^+ < 200$ (Tennekes & Lumley, 1972, p. 160). Note that the wall distance is defined as $y^+ = yu_\tau/\nu$, where y is the distance to the wall, u_τ is the frictional velocity, and ν is the viscosity of water.

As illustrated in Figure 2, the model channel has a sluice gate with a 2.54-cm opening (as an example) and five types of boundaries. The channel section upstream from the gate has a length 10 times the gate opening. The downstream channel section has a length of 17.5 cm. The types of conditions applied at the

boundaries are: 1) a water inlet at the channel's upstream end; 2) an air inlet at the upstream end; 3) an outlet at the downstream end; 4) an open boundary at the top exposed to atmospheric pressure; 5) a solid wall (or channel-bed) at the bottom.

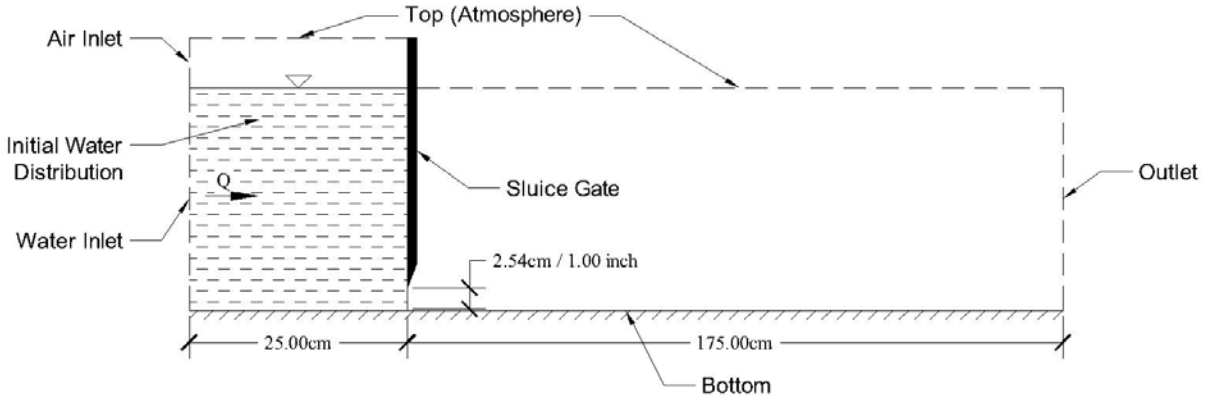

Figure 2: Setup of the model channel for numerical simulations of sluice gate flow

The solid walls (the channel-bed and gate surface) are considered to be a non-slippery boundary. They are treated using the wall function of Launder & Spalding (1983). The authors have provided details of the turbulence kinetic energy k, energy dissipation rate ε, specific rate of dissipation ω, and turbulent eddy viscosity ν_t in the logarithmic layer adjacent to a non-slippery wall.

The initial conditions for the simulations are as follows: The position of the free water surface upstream from the gate is prescribed to align with the inlet water depth. The gate is closed, and there is no water downstream from the gate. The flow velocity is zero everywhere, except at the water inlet. The pressure follows the hydrostatic distribution. The eddy viscosity is zero everywhere in the model channel. The initial values of k, ε, ω, and ν_t are derived from the experimental data, assuming that

[6] $k = \frac{3}{2}(Iu_1)^2$

[7] $\varepsilon = \frac{C_\mu^{0.75} k^{1.5}}{L}$

[8] $\omega = \frac{k^{0.5}}{C_\mu L}$

where I is the turbulence intensity (assumed as 0.5%); u_1 is the horizontal velocity at the water inlet, estimated from the flume experiments; C_μ is a constant (equal to 0.09); L is the reference length (equals to water-inlet flow depth y_1).

4 RESULTS

This section discusses the experimental and numerical results, including the contraction coefficient, contraction distance, distributed pressures, flow profile, and flow curvature. The computational results will be compared between the SST k-ω and the standard k-ε model.

4.1 Flow Profiles, Contraction Distance and Contraction Coefficient

Flow profiles downstream from the gate opening are plotted in Figure 3, for y_1/w = 8, where x/w is the longitudinal distance after the gate normalised by the gate opening, and y_2/w is the flow depth normalised also by the gate opening. The point-gauge measurements of the free surface position (the triangle, circle and square symbols) from the experiments (Table 1) show that y_2/w monotonically decreases with increasing x/w. This is true for all the three different gate openings used in the experiments (w = 2.54, 3.81, and 5.08 cm).

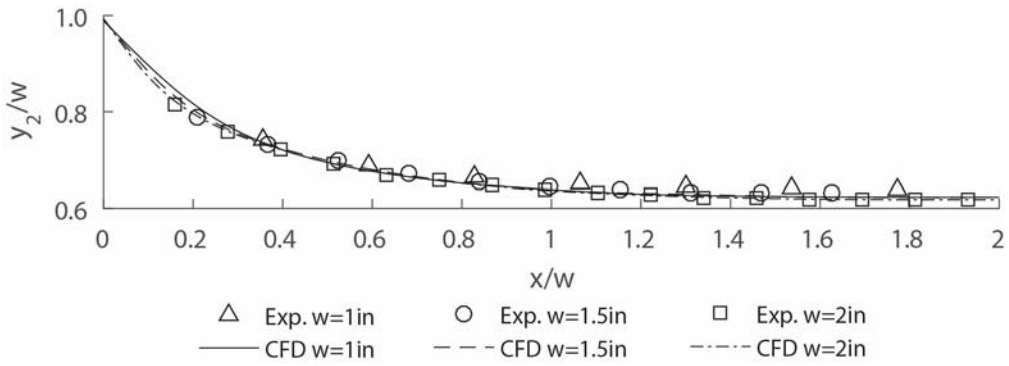

Figure 3: Measured and predicted positions of the free water surface at three different gate openings. The ratio of upstream flow depth to gate opening is $y_1/w = 8$.

It is important to note that each of the 33 data points (the symbols in Figure 3) represents the mean of the population of five experiments repeated under the same w and y_1/w conditions (Table 1), and that for each of them, the extent of variability in relation to the mean of the y_2/w population is insignificant. Quantitatively, the coefficient of variation (or the ratio of the standard deviation to the mean of the population) is in the range of 0.0033 to 0.0101 for the 33 data points. In fact, the coefficient of variation is similarly small for repeated y_2/w measurements made from each x/w location under each of the hydraulic conditions summarised in Table 1.

In Figure 3, the predicted free surface positions (the solid, dashed, and dot-dashed curves) at a state of equilibrium are shown to plot through the experimental data points. Clearly, the numerical predictions compare well with the experimental data. The results plotted in the figure correspond to the condition that the ratio of the upstream flow depth to the gate opening is $y_1/w = 8$. At other values for the ratio, ranging from $y_1/w = 4$ to $y_1/w = 16$ (Table 1), the predictions also compare well with the corresponding measurements (not shown).

Under the hydraulic conditions given in Table 1, both the measurements and predictions provide consistent details about the variations (Figure 3) of the free surface: 1) Over the longitudinal distance of the first one thirds of the gate opening (or $0 < x/w < 1/3$), the free surface drops the most rapidly with distance, which corresponds to a rapidly varied flow; 2) over the distance of the second one thirds of the gate opening (or $1/3 < x/w < 2/3$), the free surface drops significantly with distance, and the flow is also a rapidly varied flow; 3) between $x/w = 2/3$ and a threshold distance, the free surface drops gradually with distance, and the flow is a gradually varied flow. Such details have not been reported previously in the literature.

The threshold longitudinal distance, x_c, downstream from the gate opening, after which the flow becomes uniform flow of constant depth y_{2c}, is known as the contraction length. The laboratory measurements gave dimensionless contraction length $x_c/w = 1.575$, 1.470, and 1.575, for $w = 2.54$, 3.81 and 5.08 cm, respectively. The horizontal distance between two adjacent point-gauge measuring locations is 0.6 cm (much smaller than w), and the most downstream measuring location is at x/w slightly larger than two. The corresponding numerical predictions gave $x_c/w = 1.772$, 1.470, and 1.535. The predictions contain relative errors between 12.5% and -2.5%. The results of x_c/w from this paper are summarised in Table 1. They are consistent with the literature value of $x_c/w = 1.5$ (Henderson, 1966, p. 192). The gate opening has insignificant influence on the dimensionless contraction distance.

For given hydraulic conditions (Table 1), the flow depth y_{2c} at $x = x_c$ was obtained from the experiments in order to determine the contraction coefficient C_c (Equation 2). Experimental values of C_c are plotted in Figure 4 as the open triangle, circle, and square symbols, for gate opening $w = 2.54$, 3.81 and 5.08 cm (or 1, 1.5 and 2 inches), respectively. Between $w = 2.54$ and 3.81 cm, the C_c values more or less match at various values for the ratio y_1/w, seen as the filled triangle symbols overlapping filled circle symbols. The filled square symbols are plotted below the triangle and circle symbols. In other words, the C_c values drop when w increases from 3.81 cm (or 1.5 inch) to 5.08 cm (or 2 inches). The coefficient C_c appears to increase when y_1/w increases from four and approach an asymptotical value when y_1/w reaches six. The asymptotical value is 0.622 for $w = 2.54$ and 3.81 cm, and 0.618 for $w = 5.08$ cm.

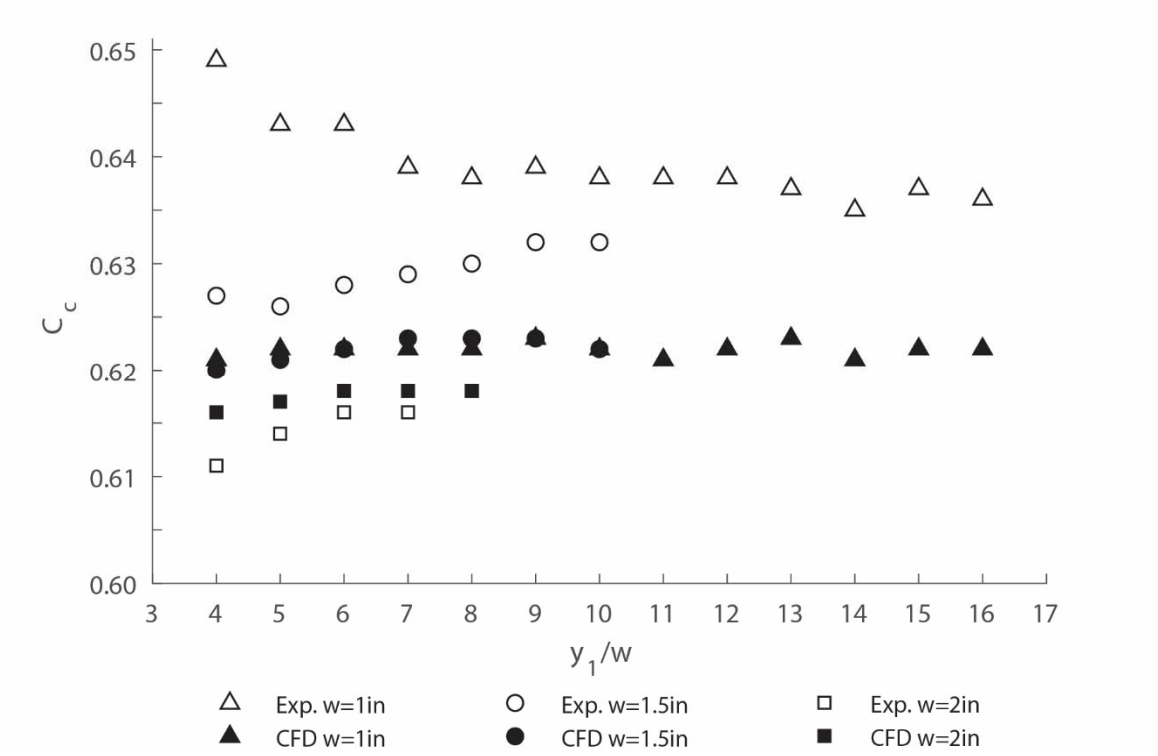

Figure 4: Contraction Coefficient C_c under Different Conditions (Table 1) of Gate Opening (w) and Upstream-Flow-Depth to Gate-Opening Ratio (y_1/w).

In Figure 4, the C_c values determined from the predicted flow depth y_{2c} at $x = x_c$ are plotted as the open triangle, circle, and square symbols, for gate opening w = 2.54, 3.81 and 5.08 cm, respectively. For w = 2.54 cm, the predictions give overestimates of C_c, in comparison to the experimental values of C_c. The overestimates for $y_1/w \leq 6$ are significant. When w increases from 2.54 to 3.81 cm, the overestimates become less significant. When w further increases to 5.08 cm, the predictions give acceptable C_c values in comparison to the experimental values.

4.2 Pressure on Sluice Gate

The measured and predicted pressures on the sluice gate surface for gate opening w = 5.08 cm are compared in Figure 5. In this figure, Z is the vertical distance above the gate's lower edge ($y_2 - w$), normalised by the elevation of the free surface above the edge ($y_1 - w$) or

[9] $Z = (y_2 - w)/(y_1 - w)$

H_{pg} is the measured or predicted pressure head, h_{pg}, normalised by ($y_1 - w$) or

[10] $H_{pg} = h_{pg}/(y_1 - w)$

which varies with position between the edge and free surface. H_{pgM} is the maximum value of H_{pg}. The maximum value of Z is equal to 0.08 for w = 2.54 cm, and 0.1 for w = 3.81 and 5.08 cm. The results (Figure 5) show little effects of the gate opening and y_1/w ratio on the distribution of pressures on the gate surface. Roth & Hager (1999) reported that H_{pg} = 0 at the lower edge (or Z = 0). In this study, H_{pg}/H_{pgM} = 0.199, 0.179, and 0.107 for w = 2.54, 3.81, and 5.08 cm, respectively. It appears that H_{pg} approaches zero as the gate opening increases. The numerical predictions are shown to compare well with experimental data.

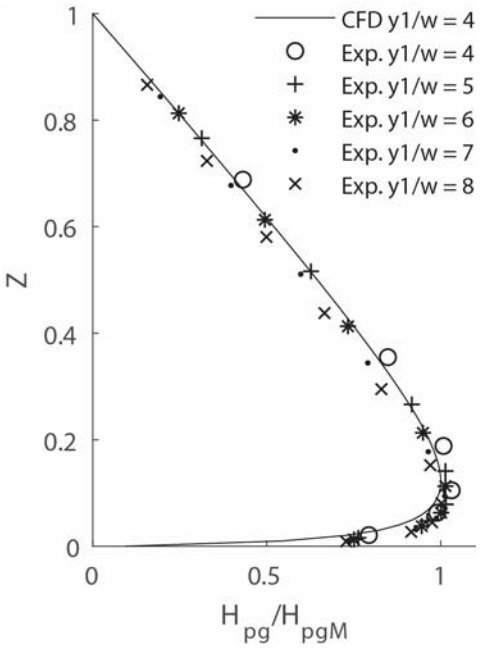

Figure 5: Distribution of Dimensionless Pressure on the Gate Surface for *w* = 5.08 cm (or 2 inches).

4.3 Pressure at the Channel-bed

This section discusses the distribution of pressure at the channel-bed based on the CFD results under the hydraulic conditions listed in Table 1. The pressure is normalised as:

[11] $H_p = \frac{h_p - h_D}{h_U - h_D}$

where h_p is the bottom pressure head; h_D is the pressure head at x/w = 5, and h_U is the pressure head at x/w = -5. These two locations are so far from the gate opening (at x = 0) that the pressures are hydrostatic (Rajaratnam & Humphries, 1982); in other words, the pressure defects at the bed is very slight. It is sufficient to discuss the pressure distribution between x/w = -3 and x/w = 3.

For each gate opening, there are no significant differences in the distributions of the dimensionless pressure given in Equation [11] among different y_1/w ratios. Thus, the distribution of averaged pressure among the y_1/w ratios is shown in Figure 6 for w = 2.54 cm (or 1 inch). The distributions for w = 3.81 and 5.08 cm (or 1.5 and 2 inches) are similar.

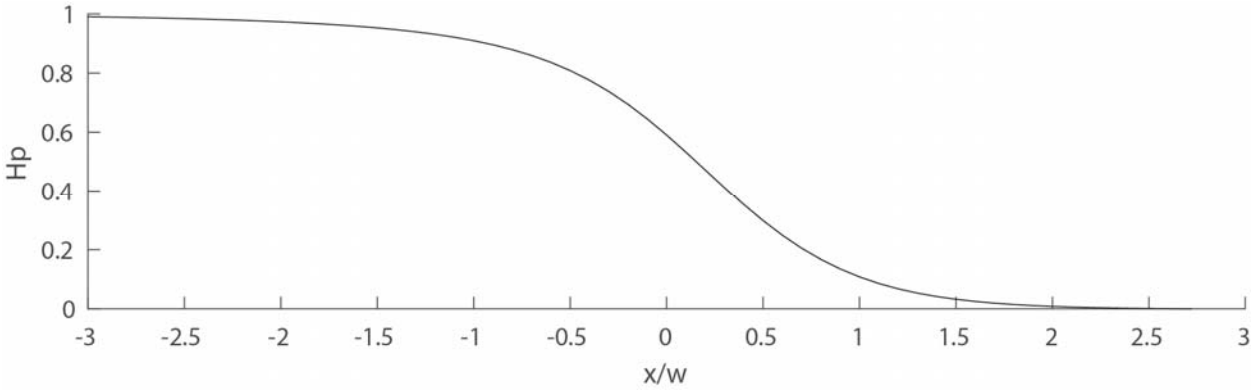

Figure 6: Distribution of Dimensionless Pressure (Equation 11) at the Channel-bed for Gate Opening w = 2.54 cm (or 1 inch).

Interestingly, at the gate opening (or x/w = 0), H_p has essential the same value for three different gate openings. At x/w = 0, the H_p values (Equation 11) for y_1/w = 4, 5, …, 16 has an mean value of $\overline{H_p}$ = 0.59 for w = 2.54 cm (or 1 inch). As listed in Table 2, the differences of these individual H_p values from the mean are very small, compared to the mean itself. Similarly, $\overline{H_p}$ is equal to 0.591 for w = 3.81 cm (or 1.5 inches), and 0.592 for w = 5.08 cm (or 2 inches). The corresponding differences are all small (Table 2). Clearly, the gate opening as well as the y_1/w have little influence on the distribution of the dimensionless pressure.

Table 2: Statistics of the Bottom Pressure at the Gate Location.

w = 1 inch				w = 1.5 inches		w = 2 inches	
y_1/w	$H_p - \overline{H_p}$	y_1/w	$H_p - \overline{H_p}$	y_1/w	$H_p - \overline{H_p}$	y_1/w	$H_p - \overline{H_p}$
4	0.005	11	0	4	0.005	4	0.005
5	0.003	12	0	5	0.003	5	0.001
6	0.001	13	-0.003	6	-0.001	6	-0.002
7	0	14	0.001	7	-0.001	7	-0.001
8	0	15	0.001	8	-0.002	8	-0.002
9	0	16	0	9	-0.002		
10	0			10	-0.002		

Regarding the differences of the individual H_p values from the mean listed in Table 2, the standard deviation σ may be used as an indicator:

[12] $\sigma = \sqrt{\frac{\sum_{i=1}^{N}(H_{pi}-\overline{H_p})^2}{N-1}}$

where N is equal to 13 for w = 2.54 cm (or 1 inch), 7 for w = 3.81 cm (or 1.5 inches), and 5 for w = 5.08 cm (or 2 inches). Calculations using Equation [12] give σ = 0.0019, 0.0028 and 0.0029, respectively.

4.4 Curvature of Downstream Flow Surface nearby Sluice Gate

In Figure 3, an example of flow profiles y_2/w versus x/w is plotted. The curvature, K, of the water surface profile can be determined as (Zill, Wright, & Cullen, 2011)

[13] $K = \frac{|F''(x)|}{[1+(F'(x))^2]^{3/2}}$

where $F'(x)$ is the first-order derivation of the flow profile; $F''(x)$ is the second-order derivation. They are evaluated as

[14] $F'(x) = \frac{F(x+\Delta x)-F(x)}{\Delta x}$

[15] $F''(x) = \frac{F'(x+\Delta x)-F'(x)}{\Delta x}$

where Δx is the spatial resolution in the longitudinal direction. The variations in K with dimensionless distance, x/w, for six gate openings were calculated. The calculations give that the curvature decreases rapidly with distance toward downward. The calculation give zero curvature at the contraction distance.

4.5 Suitability of the Turbulence Closure Models

The results discussed in previous sections of this paper have confirmed the suitability of the SST k-ω model for turbulence closure in simulations of highly curved flow after sluice gate. The use of the standard k-ε model leads to overestimates of the contraction coefficient by about 15%, compared to the experimental results. The same issue with using the k-ε model was raised in Cassan & Belaud (2012). The simulations using the k-ε model over-predicted the flow depth downstream from the gate.

5 CONCLUSION

Flow passing underneath a sluice gate has engineering relevance. In spite of extensive research of sluice gate flow conducted in the past, the characteristics of the flow immediately after the gate have not been

quantified in detail. This paper quantitatively investigates the characteristics by means of flume experiments and computer simulations. The simulations use the Reynolds-averaged Navier-Stokes equations for two-phase flow, SST k-ω model for turbulence closure, and volume of fluid method for water surface tracking. The following conclusions have been reached:

1) The CFD results of flow profile, contraction length, contraction coefficient, and pressure distribution on the gate surface compare well with the experimental data.
2) Both the experimental and numerical results show that the contraction distance is equal to 1.5 times the gate opening. This is consistent with the literature value. It has been shown that the ratio of upstream flow depth to gate opening has little effect on the dimensionless contraction length
3) The contraction coefficient has a value of 0.618 for gate opening equal to 5.08 cm. The coefficient has slightly larger values at smaller gate openings, which implies some scale effects.
4) The results of pressure show significant deviations from the hydrostatic distribution within a longitudinal distance of two times the gate opening before and after the gate. Non-hydrostatic pressure distributions prevail regardless of different values for the upstream-flow-depth to gate opening ratio, and gate opening itself.
5) The flow curvature has a maximum value at the gate opening, decreases with increasing longitudinal distance toward downstream, and diminishes at the contraction length. It has been shown that the gate opening should be 10.46 cm (or 4 inches) or larger to realistically produce flow curve that reflects field conditions.
6) The SST k-ω model provides suitable turbulence closure for simulations of highly curved flow. The standard k-ε model does not; it leads to overestimates of the contraction coefficient by about 15% for the all the hydraulic conditions covered in this paper.

6 ACKNOWLEDGEMENTS

This study received financial support from the NSERC through Discovery Grants held by S. Li.

7 REFERENCE

Cassan, L., & Belaud, G. (2012). Experimental and numerical investigation of flow under sluice gates. *Journal of Hydraulic Engineering-ASCE,* 138(4), 367-373. 10.1061/(ASCE)HY.1943-7900.0000514

Chow, V. T. (1959). *Open Channel Hydraulics*, McGraw-Hill Book Company, Inc; New York.

Frisch, M., Trucks, G., Schlegel, H. B., Scuseria, G., Robb, M., Cheeseman, J., . . . Burant, J. (2004). Gaussian 03, revision C. 02; Gaussian, Inc. *Wallingford, CT,* 26

Henderson, F. M. (1966). *Open Channel Flow, Prentice Hall, Upper Saddle River, NJ*

Launder, B. E., & Spalding, D. B. (1983). The numerical computation of turbulent flows. *Numerical Prediction of Flow, Heat Transfer, Turbulence and Combustion* (pp. 96-116) Elsevier.

Rajaratnam, N., & Humphries, J. (1982). Free flow upstream of vertical sluice gates. *Journal of Hydraulic Research,* 20(5), 427-437.

Roth, A., & Hager, W. (1999). Underflow of standard sluice gate. *Experiments in Fluids,* 27(4), 339-350.

Tennekes, H., & Lumley, J. L. (1972). *A First Course in Turbulence*, MIT Press, Cambridge, MA.

Zill, D., Wright, W. S., & Cullen, M. R. (2011). *Advanced Engineering Mathematics*, Jones & Bartlett Learning, Burlington, MA.